A wavelet-based spectral finite element for analysis of coupled wave propagation in composite beam

Mira Mitra*, S. Gopalakrishnan

Department of Aerospace Engineering, Indian Institute of Science, C.V. Raman Road, Bangalore 560012, India

Abstract

In this paper, a spectrally formulated wavelet finite element is developed and is used to study coupled wave propagation in composite beam. The formulation uses Daubechies wavelet approximation in time to reduce the governing PDE to a set of ODEs. Similar to conventional FFT-based Spectral Finite Element (FSFE) formulations, these transformed ODEs are solved using finite element (FE) techniques by deriving exact interpolation functions in the transformed domain to obtain the exact dynamic stiffness matrix. The use of the compactly supported Daubechies wavelet basis circumvents several drawbacks of the FSFE due to the required assumption of periodicity, particularly for time domain analysis. In the Wavelet-based Spectral Finite Element (WSFE) formulation, a constraint on the time sampling rate is placed to avoid spurious dispersion being introduced in the analysis. Numerical examples are presented to study wave propagation with the formulated element and emphasize the advantages of WSFE formulation over FSFE for wave propagation analysis of finite length structure. Numerical experiments are also performed to study the dispersion of waves and show the presence of spurious dispersions. Simultaneous existence of various propagating modes are graphically captured using modulated sinusoidal pulse excitation.

Keywords: Wavelet; Wave propagation; Composite beam; Finite element; Spectral finite element

1. Introduction

Wavelets have several properties that are encouraging their use for numerical solutions of partial differential equations (PDEs). The orthogonal, compactly supported wavelet basis of Daubechies [1] can provide accurate and stable representation of differential operations and also have the inherent advantage of multi-resolution analysis over the traditional methods.

Wave propagation problems deal with loading that have very high frequency content and FE formulation for such problems require large system size to capture all the higher modes. These problems are usually solved in frequency domain using Fourier methods, which can in principle achieve high accuracy in numerical differentiation. One such method is the FFT-based Spectral Finite Element Method (FSFEM) proposed by Doyle [2]. In FSFEM, first the governing PDEs are transformed to ODEs in spatial dimension using FFT in time. These ODEs are then usually solved exactly, which are used as interpolating functions for FSFE formulation. This results in exact mass distribution and hence, in absence of any discontinuity, one element is sufficient to handle 1-D structure of any length and this reduces the system size substantially.

The main drawback of the Fourier-based spectral approach is that it cannot handle waveguides of short lengths. This is because, short length forces multiple reflections at smaller time scales. Since Fourier transforms are associated with a finite time window (that depends on time sampling rate), shorter lengths of waveguide do not allow the response to die down within the chosen time window, irrespective of the type of damping used in modeling. This forces the response to wrap around, that is the remaining part of the response beyond the chosen time window, will start appearing first and this totally distorts the response. It is in such cases, compactly supported wavelets, which have localized basis functions can be efficiently used for waveguides of short lengths.

The present Wavelet-based Spectral Finite Element Method (WSFEM) follows an approach very similar to FSFEM, except that Daubechies scaling functions are

* Corresponding author. Tel.: +91 (80) 2293 2438; E-mail: mira@aero.iisc.ernet.in

Computational Fluid and Solid Mechanics 2005
K.J. Bathe (Editor)

used for approximation in time for reduction of PDEs to ODEs. WSFE can be formulated assuming periodic boundary condition and for this case the results are expected to be similar to those obtained using FSFEM [3]. However, an extrapolation technique proposed by Amaratunga and Williams [4] can be used for adapting wavelet in a finite domain and imposition of initial values. The latter approach can remove the problem associated with 'wrap around' in FSFEM and thus result in smaller time window for the same problem. Further, as a consequence, WSFEM can be used for finite length undamped structures where FSFEM does not work well.

In composite beams, due to high ratios of elastic moduli, the effect of neglecting higher order modes like shear and lateral contraction is non-negligible. Thus higher order beam model is essential for accurate analysis, particularly for beams with strong asymmetry. In this paper, WSFE is formulated for a coupled composite beam with axial, bending, shear and contractional degree of freedom. FSFE for such composite beam has been formulated by Mahapatra and Gopalakrishnan [5].

Though FSFEM encounters several problems in time domain wave propagation analysis, it is extensively used to study the various frequency dependent characteristics of waves i.e the spectrum and dispersion relations can be obtained directly from analysis in the transformed ODEs. In this paper, a correspondence is established between the transformed ODEs in periodic WSFEM with those obtained in FSFEM and the formulated WSFE is directly used for such frequency domain analysis of coupled wave propagation in laminated composite beam.

The paper is organized as follows. In Section 2, the details of WSFE for composite beam is presented. Following this a section on numerical examples is provided to study spectrum relation and wave propagation due broad band and modulated excitations. In all the cases comparison is provided with corresponding FSFEM results. The paper ends with some important conclusions.

2. Formulation

The first step in the formulation of WSFE is the reduction of the governing differential wave equations to ODEs using Daubechies scaling functions for approximation in time. The details of Daubechies orthogonal compactly supported wavelets are given in [1]. The governing equations for composite beam derived in [5] are

$$I_0\frac{\partial^2 u}{\partial t^2}-I_1\frac{\partial^2\phi}{\partial t^2}-A_{11}\frac{\partial^2 u}{\partial x^2}+B_{11}\frac{\partial^2\phi}{\partial x^2}-A_{13}\frac{\partial\psi}{\partial x}=0 \tag{1}$$

$$I_2\frac{\partial^2\psi}{\partial t^2}+I_1\frac{\partial^2 w}{\partial t^2}+A_{13}\frac{\partial u}{\partial x}-B_{13}\frac{\partial\phi}{\partial x}+A_{33}\psi- B_{55}\left(\frac{\partial^2 w}{\partial x^2}-\frac{\partial\phi}{\partial x}\right)-D_{55}\frac{\partial^2\psi}{\partial x^2}=0 \tag{2}$$

$$I_0\frac{\partial^2 w}{\partial t^2}+I_1\frac{\partial^2\psi}{\partial t^2}-A_{55}\left(\frac{\partial^2 w}{\partial x^2}-\frac{\partial\phi}{\partial x}\right)-B_{55}\frac{\partial^2\psi}{\partial x^2}=0 \tag{3}$$

$$I_2\frac{\partial^2\phi}{\partial t^2}-I_1\frac{\partial^2 u}{\partial t^2}-A_{55}\left(\frac{\partial w}{\partial x}-\phi\right)-B_{55}\frac{\partial\psi}{\partial x}+ B_{11}\frac{\partial^2 u}{\partial x^2}-D_{11}\frac{\partial^2\phi}{\partial x^2}+B_{11}\frac{\partial\psi}{\partial x}=0 \tag{4}$$

$u(x, t)$, $w(x, t)$, $\phi(x, t)$ and $\psi(x, t)$ are the axial, transverse, shear and contractional displacements respectively. The stiffness and inertia constants in Eq. (1)–(4) has the usual meaning and the details are given in [5].

Let $\tau = 0, 1, \ldots, n-1$ be the sampling points, then

$$t=\Delta t\tau \tag{5}$$

where, Δt is the time interval between two sampling points. The function $u(x, t)$ can be approximated by scaling function $\varphi(\tau)$ at an arbitrary scale as

$$u(x,t)=u(x,\tau)=\sum_k u_k(x)\varphi(\tau-k),\quad k\in\mathbf{Z} \tag{6}$$

where, $u_k(x)$ (referred as u_k hereafter) are the approximation coefficient at a certain spatial dimension x. The other displacements $w(x, t)$, $\phi(x, t)$, $\psi(x, t)$ can be transformed similarly and Eq. (1) can be written as

$$\frac{I_0}{\Delta t^2}\sum_k u_k\varphi''(\tau-k)-\frac{I_1}{\Delta t^2}\sum_k\phi_k\varphi''(\tau-k)+ \sum_k\left(-A_{11}\frac{d^2u_k}{dx^2}+B_{11}\frac{d^2\phi_k}{dx^2}-A_{13}\frac{d\psi_k}{dx}\right)\varphi(\tau-k)=0 \tag{7}$$

Taking the inner product on both sides of Eq. (7) with $\varphi(\tau - j)$, where $j = 0, 1, \ldots, n-1$ and using the orthogonality of the translates of scaling functions, i.e.

$$\int\varphi(\tau-k)\varphi(\tau-j)d\tau=0\ \text{ for }\ j\neq k \tag{8}$$

Equation (7) can be written as

$$\frac{1}{\Delta t^2}\sum_{k=j-N+2}^{j+N-2}\Omega^2_{j-k}(I_0u_k-I_1\phi_k)-A_{11}\frac{d^2u_j}{dx^2}+B_{11}\frac{d^2\phi_j}{dx^2}- A_{13}\frac{d\psi_j}{dx}=0\ j=0,\ 1,\ \ldots,\ n-1 \tag{9}$$

where N is the order of the Daubechies wavelet and $\Omega^2{}_{j-k}$ are the connection coefficients defined as

$$\Omega^2_{j-k} = \int \varphi''(\tau - k)\varphi(\tau - j)d\tau \tag{10}$$

The details for evaluation of connection coefficients for different orders of derivative is given in [6]. While dealing with finite length data sequence, problems arise at the boundaries. It can be observed from the ODEs given by Eq. (9) that certain coefficients (u_j) near the vicinity of the boundaries ($j = 0$ and $j = n - 1$) lie outside the time window [0 t_f] defined by $j = 0, 1, \ldots, n - 1$. Several approaches for treating boundaries are reported in the literature. Here, first a circular convolution method is adopted assuming periodicity of the solution. Next, the wavelet based extrapolation scheme [4] is implemented for solution of boundary value problems. This approach allows treatment of finite length data and uses polynomial to extrapolate coefficients at boundaries either from interior coefficients or boundary values. The method is particularly suitable for approximation in time for the ease to impose initial values.

However, either of the above methods converts the ODEs in Eq. (9) to a coupled matrix equation of the form

$$[\Lambda^2](I_0\{u_j\} - I_1\{\phi_j\}) - A_{11}\{\frac{d^2u_j}{dx^2}\} + B_{11}\{\frac{d^2\phi_j}{dx^2}\} - A_{13}\{\frac{d\psi_j}{dx}\} = 0 \tag{11}$$

$[\Lambda^2]$ is the connection coefficient matrix corresponding to Ω^2_{j-k} and is different for periodic and non periodic solutions. Though $[\Lambda^2]$ and $[\Lambda^1]$ for second and first order derivative can be derived independently, in the present formulation, $[\Lambda^2] = [\Lambda^1]^2$ for imposition of initial values. The above coupled Eq. (11) can be decoupled by eigenvalue analysis of $[\Lambda^1]$ as

$$[\Lambda^1] = [\Gamma][\Pi][\Gamma]^{-1} \tag{12}$$

where, $[\Pi]$ is the diagonal matrix containing the diagonal terms $i\beta_j$ and $[\Gamma]$ is the eigenvector matrix, $i = \sqrt{-1}$ and β_j is given by

$$\beta_j = -\frac{2}{\Delta t}\sum_{k=1}^{N-2}\Omega^1_k \sin\left[\frac{2\pi kj}{n}\right] \qquad j = 0, 1, \ldots, n-1 \tag{13}$$

Thus Eq. (11) can be written as

$$-I_0\beta_j^2\hat{u}_j + I_1\beta_j^2\hat{\phi}_j - A_{11}\frac{d^2\hat{u}_j}{dx^2} + B_{11}\frac{d^2\hat{\phi}_j}{dx^2} - A_{13}\frac{d\hat{\psi}_j}{dx} = 0 \tag{14}$$

where, $\hat{u}_j$ and similarly other transformed displacements are $\hat{u}_j = [\Gamma]^{-1}u_j$. Following the above steps, the other three governing differential equations (2–4) can be transformed as

$$-I_2\beta_j^2\hat{\psi}_j - I_1\beta_j^2\hat{w}_j + A_{13}\frac{d\hat{u}_j}{dx} - B_{13}\frac{d\hat{\phi}_j}{dx} + A_{33}\hat{\psi}_j - B_{55}\left(\frac{d^2\hat{w}_j}{dx^2} - \frac{d\hat{\phi}_j}{dx}\right) - D_{55}\frac{d^2\hat{\psi}_j}{dx^2} = 0 \tag{15}$$

$$-I_0\beta_j^2\hat{w}_j - I_1\beta_j^2\hat{\psi}_j - A_{55}\left(\frac{d^2\hat{w}_j}{dx^2} - \frac{d\hat{\phi}_j}{dx}\right) - B_{55}\frac{d^2\hat{\psi}_j}{dx^2} = 0 \tag{16}$$

$$-I_2\beta_j^2\hat{\phi}_j - I_1\beta_j^2\hat{u}_j - A_{55}\left(\frac{d\hat{w}_j}{dx} - \hat{\phi}_j\right) - B_{55}\frac{d\hat{\psi}_j}{dx} + B_{11}\frac{d^2\hat{u}_j}{dx^2} - D_{11}\frac{d^2\hat{\phi}_j}{dx^2} + B_{11}\frac{d\hat{\psi}_j}{dx} = 0 \tag{17}$$

The form of the transformed equations Eqs. (14)–(17) is the same as those in FSFEM and thus the remaining part of WSFE formulation for composite beam will be exactly similar to FSFE formulation described in [5].

2.1 Frequency domain analysis

Though periodic WSFE solution encounters all the problems of FSFEM in time domain analysis it allows the derivation of a relation between the transformed ODEs in WSFEM with those in FSFEM. This leads to the direct use of WSFE for frequency domain analysis similar to FSFE.

For periodic solution, the wavelet transformation can be written as the matrix equation [7]

$$\begin{bmatrix} U_0 \\ U_1 \\ U_2 \\ \vdots \\ \vdots \\ \vdots \\ U_{n-1} \end{bmatrix} = \begin{bmatrix} 0 & 0 & 0 & \cdots & \varphi_{N-2} & \cdots & \varphi_2 & \varphi_1 \\ \varphi_1 & 0 & 0 & \cdots & 0 & & \varphi_3 & \varphi_2 \\ \varphi_2 & \varphi_1 & 0 & \cdots & 0 & & \varphi_4 & \varphi_3 \\ \vdots & \vdots & \vdots & \cdots & \vdots & \cdots & \vdots & \vdots \\ \varphi_{N-2} & \varphi_{N-3} & \varphi_{N-4} & \cdots & & & 0 & 0 \\ \vdots & \vdots & \vdots & \cdots & \vdots & \cdots & \vdots & \vdots \\ 0 & 0 & 0 & \cdots & \varphi_{N-3} & \cdots & \varphi_1 & 0 \end{bmatrix} \begin{bmatrix} u_0 \\ u_1 \\ u_2 \\ \vdots \\ \vdots \\ \vdots \\ u_{n-1} \end{bmatrix} \tag{18}$$

where U_j, φ_j are the values of $u(x,\tau)$ and $\varphi(\tau)$ at $\tau = j$. As described by Amaratunga et al. [7], for such circulant matrix the Eq. (18) can be replaced by a convolution relation, which can be written as

$$\{\tilde{U}_j\} = \{\tilde{K}_{\varphi j}.\tilde{u}_j\} \tag{19}$$

$$\{\tilde{u}_j\} = \{\tilde{U}_j/\tilde{K}_{\varphi j}\} \tag{20}$$

where $\{\tilde{U}_j\}$, $\{\tilde{u}_j\}$ are FFT of $\{U_j\}$, and $\{u_j\}$ respectively (similar relations hold for other displacements). $\tilde{K}_\varphi$ is FFT of first column $K_\varphi = \{0\ \varphi_1\ \varphi_2 \ldots \varphi_{N-2} \ldots 0\}$ of the scaling function matrix in Eq. (18). Similarly the connection coefficient matrix $[\Lambda^1]$ is also a circulant matrix and thus Eq. (11) can be written as

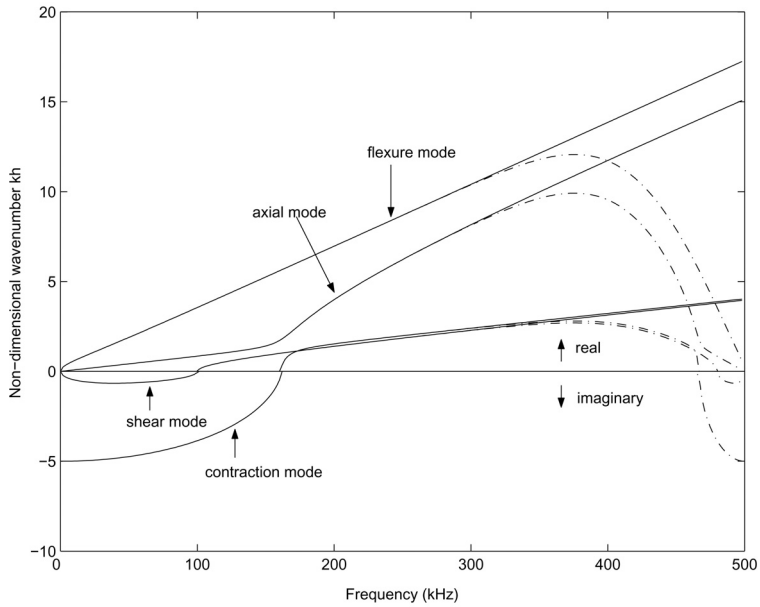

Fig. 1. Spectrum relation for graphite-epoxy [0_4] beam: (– · –) WSFEM and (—) FSFEM.

$$I_0\left\{\tilde{K}^2_{\Omega j}\cdot\tilde{u}_j\right\} - I_1\left\{\tilde{K}^2_{\Omega j}\cdot\tilde{\phi}_j\right\} - A_{11}\{\frac{d^2\hat{u}_j}{dx^2}\} + B_{11}\{\frac{d^2\tilde{\phi}_j}{dx^2}\} - A_{13}\{\frac{d\tilde{\psi}_j}{dx}\} = 0 \tag{21}$$

where, $\tilde{K}_{\Omega j}$ are the FFT coefficients of the first column of $[\Lambda^1]$ given as $K_\Omega = \{\Omega^1_0 \;\; \Omega^1_{-1} \;\; \ldots \;\; \Omega^1_{-N+2} \cdots \Omega^1_{N-2} \cdots \Omega^1_1\}$. It can be easily shown that the FFT coefficients $\tilde{K}_{\Omega j}$ are equal to the eigenvalues $i\beta_j$ of the matrix $[\Lambda^1]$.

Substituting Eq. (20) in Eq. (21) and multiplying by $\tilde{K}_{\varphi j}$ on both sides we get

$$I_0\left\{\tilde{K}^2_{\Omega j}\tilde{U}_j\right\} - I_1\left\{\tilde{K}^2_{\Omega j}\tilde{\Phi}_j\right\} - A_{11}\{\frac{d^2\tilde{U}_j}{dx^2}\} + B_{11}\{\frac{d^2\tilde{\Phi}_j}{dx^2}\} - A_{13}\{\frac{d\tilde{\psi}_j}{dx}\} = 0 \tag{22}$$

$$-I_0\beta_j^2\tilde{U}_j + I_1\beta_j^2\tilde{\Phi}_j - A_{11}\{\frac{d^2\tilde{U}_j}{dx^2}\} + B_{11}\{\frac{d^2\tilde{\Phi}_j}{dx^2}\} - A_{13}\{\frac{d\tilde{\psi}_j}{dx}\} = 0, \quad j = 0,\ 1,\ \ldots,\ n-1 \tag{23}$$

In FSFEM, the transformed ODEs are of same form except β_j are replaced with ω_j given as

$$\omega_j = \frac{2\pi j}{n\Delta t} \tag{24}$$

It can be seen that for a given sampling rate Δt, β_j exactly matches ω_j up to a certain fraction of Nyquist frequency $f_{nyq} = \frac{1}{2\Delta t}$. Thus, similar to FSFE, WSFE can be used directly for studying frequency dependent characteristics such as spectrum and dispersion relations, but only up to a certain fraction of f_{nyq}, depending on the order of basis.

For non-periodic solution, unlike periodic WSFE, the β_j is complex with the real part being equal to those in periodic solution.

3. Numerical experiments

All the numerical experiments presented are performed on AS4/3501–6 graphite-epoxy composite beam with four plies. The beam has a depth of $h = 0.01$ m and width $b = 0.01$ m. First, WSFEM is used to study the spectrum relation of the beam for all the four modes. Next, the formulated WSFE is used to study wave propagation in finite length coupled beam. In both the cases, the results are compared with those obtained using FSFEM. Finally, the response of the beam to modulated sinusoidal pulse showing all the four propagating modes is presented.

In Fig. 1, the wavenumbers for a [0_4] beam, computed using periodic WSFEM (k_w) with $N = 24$ are plotted for all the four modes i.e. axial, flexural, shear and contractional and compared with those obtained using FSFEM (k_f). The sampling rate $\Delta t = 1$ μs and corresponding Nyquist frequency $f_{nyq} = 500$ kHz. It can be seen that all the k_w matches exactly with k_f up to a certain fraction (approximately 0.6 here) of f_{nyq} beyond

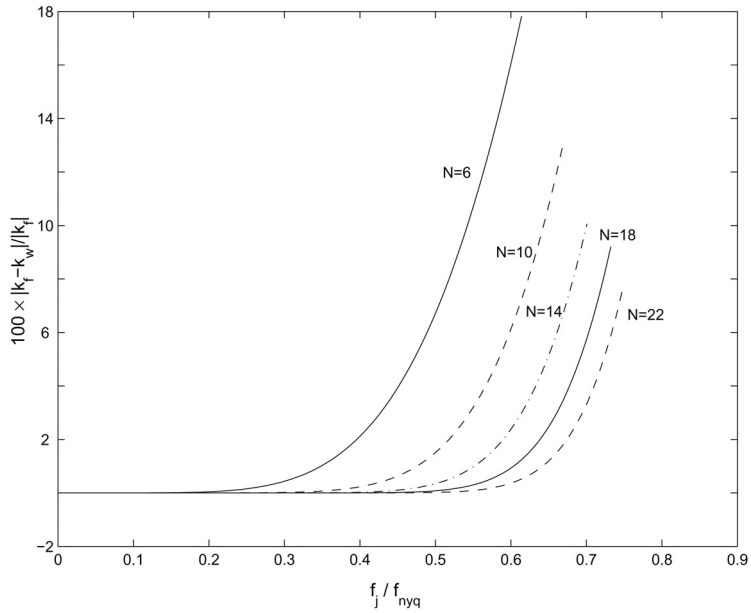

Fig. 2. Comparison of wavenumbers k_f (FSFEM) and k_w (WSFEM) for different order (N) of basis.

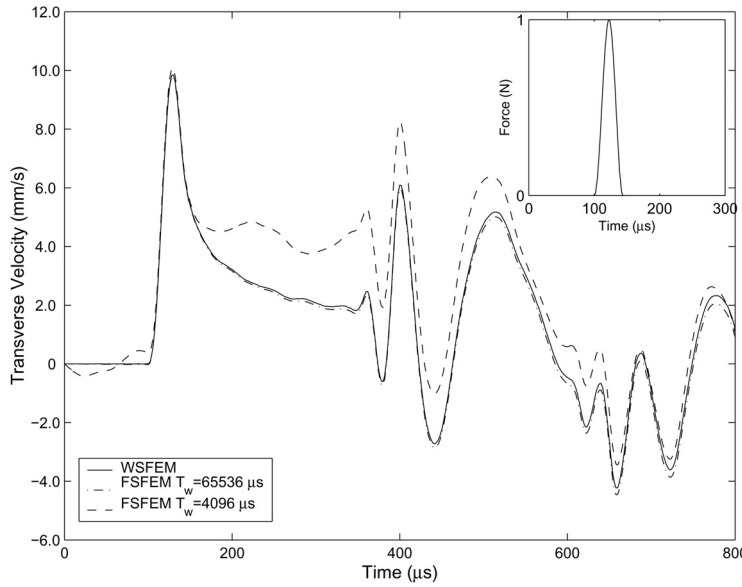

Fig. 3. Transverse tip velocity in a graphite-epoxy $[0_2/60_2]$ beam due to impulse bending load applied at tip (time history of load is shown in inset).

which, we can see spurious dispersion. This fraction depends only on N, and in Fig. 2 the percentage error in the form of $\frac{|k_f - k_w|}{|k_f|}$ is plotted with respect to the fraction of f_{nyq} for different N. Moreover, in WSFEM, the Δt should be such that the frequency content of the loading should be within this allowed frequency range to obtain accurate results. The imposition of boundary conditions for non-periodic WSFE solution adds an imaginary (real) part to the wavenumber while the real (imaginary) part is same as that of periodic WSFEM.

Figure 3 shows the transverse tip velocity in a cantilever beam due to unit impulse load applied at tip. The

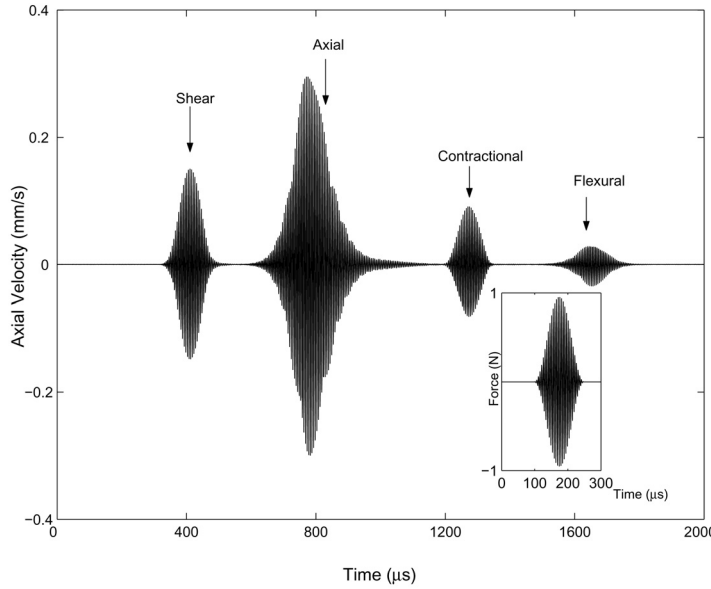

Fig. 4. Axial velocity of graphite-epoxy $[0_2/60_2]$ beam due to sinusoidal pulse modulated at 200 kHz applied in transverse direction (time history of load is shown in inset).

unit impulse load has a duration of 50 μs and frequency content 44 kHz. The time history of the load is given as an inset in Fig. 3. The beam has a ply layup of $[0_2/60_2]$ and length $L = 0.25$ m. As discussed earlier, although WSFEM can be efficiently used for wave propagation analysis of undamped finite length structures, in comparison with FSFEM, which does not work for such structures, a damping of $\eta = 0.1$ (see Doyle [2]) is considered. Both WSFEM and FSFEM require a single element to predict the results which validates the exactness of the dynamic stiffness matrices. For the WSFEM result, the time window $T_w = 1024$ μs, the sampling rate $\Delta t = 2$ μs and the order of basis $N = 24$. This result has been compared with FSFEM results for different T_w. It can be seen that the FSFEM result for $T_w = 4096$ μs is highly distorted due to 'wrap around'. These distortions decrease with increasing T_w to 65536 μs and matches well with WSFEM results.

Figure 4 shows the axial response due to modulated sinusoidal pulse at 200 kHz (time history of the load is shown in inset of Fig. 4) applied in transverse directions. The load is applied at a point on an infinite $[0_2/60_2]$ beam and the response is measured at a point 2 m from the point of application. For the above asymmetric ply configuration a coupling exists between all the four modes. It can be seen from Fig. 1 that the shear and contractional modes propagate only after a certain cut-off frequency ($\approx$ 95 kHz for shear and $\approx$ 160 kHz for contractional mode [5]). The loading frequency considered here is higher than these frequencies and thus all the four coupled non-dispersive modes are captured simultaneously. The extent of coupling can also be graphically interpreted from Fig. 4. The results are obtained using periodic WSFEM with $\Delta t = 1$ μs and $N = 24$. The reason behind choosing $\Delta t = 1$ μs is that for this sampling rate, spurious dispersion is not encountered within the frequency range of loading (i.e. 200 kHz). WSFEM with increased $\Delta t = 2$ μs will not be able to simulate the accurate wave propagation.

4. Conclusions

This paper presents the formulation and validation of wavelet based spectral element for coupled wave propagation analysis in composite beam. The novelty of the spectral element developed is that it uses wavelet transform to reduce the PDEs to ODEs unlike FFT in conventional spectral element formulation. The present method proves to be more efficient as it removes several problems associated with FSFEM for time domain analysis. In this paper, WSFEM is also used for frequency domain analysis. Based on this analysis, the sampling rate required in WSFEM can be a-priori determined depending on the excitation frequency and order of wavelet basis. Numerical experiments presented highlight these advantages and limitations of WSFE in comparison to FSFE, for time and frequency domain analysis respectively.

References

[1] Daubechies I. Ten lectures on wavelets. CBMS-NSF Series in Applied Mathematics. Philadelphia, PA: SIAM, 1992.
[2] Doyle JF. Wave Propagation in Structures. New York: Springer, 1999.
[3] Mitra M, Gopalakrishnan S. Spectrally formulated wavelet finite element for wave propagation and impact force identification in connected 1-D waveguides. Int J Solids Struct (accepted).
[4] Amaratunga K, Williams JR. Wavelet-Galerkin solution of boundary value problems. Arch Comput Methods Eng 1997;4(3):243–285.
[5] Mahapatra DR, Gopalakrishnan S. A spectral finite element model for analysis of axial-flexural-shear coupled wave propagation in laminated composite beams. Composite Struct 2003;59(1):67–88.
[6] Beylkin G. On the representation of operators in bases of compactly supported wavelets. SIAM J Numer Anal 1992;6(6):1716–1740.
[7] Amaratunga K, Williams JR, Qian S, Weiss J. Wavelet-Galerkin solutions for one-dimensional partial differential equations. Int J Numer Methods Eng 1994;37:2703–2716.